Simultaneous identification of excitation time histories and parametrized structural damages

Q. Zhang[a,b,c,*], Ł. Jankowski[b], Z. Duan[d]

[a] *College of Civil and Architecture Engineering, Dalian Nationalities University, Dalian 116600, P. R. of China*
[b] *Smart-Tech Centre, Institute of Fundamental Technological Research (IPPT PAN), Warsaw, Poland*
[c] *School of Civil Engineering, Harbin Institute of Technology, Harbin 150090, P. R. of China*
[d] *Harbin Institute of Technology Shenzhen Graduate School, Shenzhen 5180553, P. R. of China*

Abstract

This paper presents and experimentally verifies an effective method for simultaneous identification of excitations and damages, which are two crucial factors in structural health monitoring and which often coexist in practice. The unknowns are identified by minimizing a time-domain square distance between the measured and the computed responses. Even though both damage and excitation are unknown, only damage parameters are treated here as the optimization variables: given the damage, the excitation is uniquely determined from the measured responses. As a result, all unknowns are of the same type, which allows standard optimization algorithms to be used and obviates the need for two-step procedures. The sensitivity analysis is facilitated by interpolating in each iteration the relation between structural responses and damage parameters. The numerical costs are further decreased by the fast reanalysis approach of the virtual distortion method (VDM), which is used to compute exact impulse responses of the damaged structure. The proposed methodology is verified both numerically (using a multi-span frame) and experimentally (using a cantilever beam). Stiffness-related damages and mass-related modifications are identified successfully together with the three tested types of external excitation.

Keywords: Structural health monitoring, Load identification, Damage identification, Virtual distortion method (VDM)

1. Introduction

Loads and damages are two important factors in structural health monitoring (SHM). The effectiveness of the related monitoring techniques is crucial for maintaining structural integrity and can provide indispensable evidence in forensic engineering. Over the recent years, the respective identification problems have become widely researched fields and several robust methods have been proposed. However, the problems are almost always treated as decoupled: either the external excitations are assumed to be known or to belong to a well-defined class (and the damage is identified) or the structure is assumed to be known (to identify the excitations). Although such an approach can be problematic in applications, where unknown damages and unknown arbitrary excitations coexist, together influence the structural response and are both of interest, it seems that the research on simultaneous identification of arbitrary excitations and damages is very limited.

Damage identification is the primary task of most of SHM systems. In general, there are two fundamental groups of methods: high-frequency local NDT (non-destructive testing) methods and low-frequency global SHM approaches. The NDT methods are used for local detection and precise identification of defects in narrow inspection zones around the instrumentation; they rely on ultrasonic [1, 2] or statistical classification

*Corresponding author. Tel.: +86 411 87656272; fax: +86 411 87618179.
Email addresses: zhangqingxia_hit@hotmail.com (Q. Zhang), ljank@ippt.gov.pl (Ł. Jankowski), duanzd@hit.edu.cn (Z. Duan)

techniques [3]. These methods are usually costly in application, do not require structural modeling and are outside the scope of this paper. Global SHM methods are aimed at remote identification of damages via an automated analysis of global structural response; in order to be detectable, the damages must be significant enough to affect the global response. In [4], the SHM methods are categorized into model-based and pattern matching approaches. Others [5] single out modal methods [6], time domain methods [7] and wavelet methods [8]. A part of the SHM methods rely on the assumption that the external loads are well-defined and known, while others (like most of modal and time series methods) assume the excitation to belong to a specified class with well-defined characteristics (e.g. ambient excitation or impulse load). As a result, generalization to the case of an unknown arbitrary excitation is usually not possible.

Most of the techniques used for off-line *load identification* are reviewed in [9, 10, 11]. They are applied in time domain [12, 13], frequency domain [14, 15] or sometimes wavelet domain [16]. Online load identification is usually performed using observer techniques [17, 18], the Inverse Structural Filter (ISF) [19, 20] or Kalman filter [21]. All these methods are model-based and rely on the accuracy of the available numerical model of the monitored structure. Another group of load identification methods, like [8, 22], is based on computational intelligence techniques and belong to the class of pattern recognition approaches; thus, they also require a definite structure in order to build the load-response patterns for initial learning. Generalization to structures with unknown damages does not seem to be straightforward and is, as a rule, not considered.

Therefore, if unknown arbitrary excitations and structural damages coexist, the related identification problems are inherently coupled: it is in general not possible to solve them independently of each other. Due to the essentially different natures of both types of unknowns, a two-step iteration procedure is often adopted: the excitations and structural parameters are updated separately in each iteration, so that the optimization process proceeds in an alternate manner. Chen and Li [23] propose a method based on an iterative least-squares identification procedure, which requires each degree of freedom (DOF) of the monitored structure to be instrumented. Zhu and Law [24] propose a method for simultaneous identification of moving forces and damages in simply-supported beams, where the excitation models a moving vehicular load. The required number of sensors is one less than the number of the beam elements. A method based on sensitivity of structural responses is proposed and experimentally verified by Lu and Law [25]. The unknown non-moving force is represented in the form of a sum of a constant and sinusoidal terms. The parameters of the force (amplitudes and frequencies) are identified along the damage (modifications of element stiffnesses) with a limited number of measurements.

In principle, parametrization of the unknown force allows the parameters related to the damage and excitation to be updated simultaneously in each iteration. Moreover, it can significantly improve conditioning of the identification problem and reduce the number of required sensors. This is the approach pursued by Zhang et al., which present in [26] a method for simultaneous identification of structural damage and support excitation that is modeled using a finite series of Chebyshev polynomials; their amplitudes are treated as the optimization variables along with the stiffness modification coefficients. Similarly, Hoshiya and Maruyama [27] apply a weighted global iteration procedure and the extended Kalman filter for simultaneous identification of a moving load and modal parameters of a simply supported beam. The load is parametrized by its magnitude and velocity (a constant moving force) or static magnitude, velocity, damping and frequency (a moving single DOF oscillator). In [28], Zhang et al. propose a method for simultaneous identification of local damages and multiple moving masses. Thanks to the parametrization of the unknown loads, these methods can treat all the unknowns in a unified manner and do not require two-step identification procedures. A different approach, based on the virtual distortion method (VDM, [4, 7]), is proposed by Zhang et al. in [29]. The damages are modeled by virtual distortions, which are equivalent to locally applied pseudo-loads and are directly identified along with the unknown excitation forces using standard load identification procedure. As a result, strain-stress relationships of the damaged elements can be recovered and used to identify not only the extent but also the type of the damage, which thus need not be assumed in advance. The cost is the large number of sensors, which cannot be smaller than the number of excitations plus the number of virtual distortions that model the damages.

This paper proposes a new approach for simultaneous identification of structural damages (defined as local modifications of structural stiffness and mass) and unknown arbitrary excitation forces. The approach can be characterized as follows:

- Damage parameters are the only optimization variables. The excitation is not treated as an independent optimization variable: given damage parameters, it is uniquely determined from the measured structural response. A limited number of sensors is thus required, which nevertheless must exceed the number of the unknown excitations. Moreover, all the unknowns are of the same type, which obviates the need for relatively cumbersome two-step optimization procedures and alternate updating of damage- and excitation-related unknowns.

- Given the damage parameters, the exact impulse responses of the modified structure are obtained through a fast reanalysis process based on the VDM. The number of full simulations of the modified structure is thus significantly reduced.

- In each iteration, the structural response is interpolated based on few initially computed exact impulse-responses. As a result, (1) the number of actual load identifications as well as the total number of iterations are both decreased, which further reduces the computational cost, and (2) sensitivity analysis is significantly facilitated, which is important especially in the case of ill-conditioning and numerical regularization. Standard gradient- and Hessian-based optimization algorithms can be used.

Besides the above measures, a moving time window technique and parametrization of the time-history of unknown excitations are employed in order to further reduce the computational cost and improve the conditioning of the problem.

The next section reformulates the VDM into the form that suits the considered problem; for other formulation in frequency domain see [30]. The proposed identification method is introduced in the third section and verified in the numerical example and the experiment presented in the fourth and fifth sections.

2. Virtual distortion method (VDM)

The virtual distortion method (VDM) is a quick reanalysis method [31], applicable in static and dynamic analysis of structures [7, 30]: given the response of the intact structure, the VDM allows the response of the damaged structure to be quickly computed without a time-consuming full structural simulation.

Within the framework of the finite element method (FEM), the VDM models damages of a finite element with the equivalent pseudo-loads that are applied in its degrees of freedom (DOFs). This is always possible, as the effect of any modification of a finite element is transferred to the neighboring elements only through its internal nodal forces. In particular, mass modifications are modeled via unequilibrated pseudo-loads. In case of a stiffness-related damage, the equivalent pseudo-loads are equilibrated and can be more naturally represented in the form of virtual distortions (intentionally introduced additional strains) of the affected element. The intact structure is assumed to be linear, as any potential nonlinearities are modeled using the VDM.

As a result, instead of a damaged structure subjected to an external excitation, the VDM considers the intact linear structure subjected to certain pseudo-loads and the same external excitation. Both structures are equivalent in terms of the displacement/acceleration response. Therefore, the response of the damaged structure is represented by a sum of the responses of the intact structure to (1) the same external load and (2) the imposed pseudo-loads (virtual distortions), see Eq. (14). The response is thus expressed solely in the terms of certain local characteristics of the original unmodified structure, which can be either precomputed or even directly measured [32]. As a result, time-consuming repeated updating and simulations of the finite element (FE) model are avoided.

This paper considers only stiffness- and mass-related damages. The methodology can be straightforwardly extended to include other damage patterns and physical nonlinearities like breathing cracks [28] or material yielding [13, 7], but geometric linearity (assumption of small deformations) is required.

2.1. Distortions of a finite element

For a finite element, the number and forms of its distortions can be analyzed using the eigenvalue problem of its local stiffness matrix $\mathbf{K}_i$, where i stands for the ith element. The matrix is positive semi-definite,

hence the eigenvectors are of two kinds only: unit distortion vectors that correspond to positive eigenvalues and unit rigid motion vectors that correspond to zero eigenvalues. The matrix $\mathbf{K}_i$ can be expressed in terms of its positive eigenvalues λ_{ij} and the corresponding eigenvectors $\boldsymbol{\varphi}_{ij}$,

$$\mathbf{K}_i = \sum_j \lambda_{ij} \boldsymbol{\varphi}_{ij} \boldsymbol{\varphi}_{ij}^{\mathrm{T}}. \tag{1}$$

The eigenvector $\boldsymbol{\varphi}_{ij}$ represents the jth *unit distortion* of the ith finite element and corresponds to the following local nodal load:

$$\mathbf{n}_{ij} = \mathbf{K}_i \boldsymbol{\varphi}_{ij} = \lambda_{ij} \boldsymbol{\varphi}_{ij}. \tag{2}$$

Given the vector $\mathbf{u}_i(t)$ of local nodal displacements, the corresponding *total distortions* $\kappa_{ij}(t)$ of the element can be computed as

$$\kappa_{ij}(t) = \boldsymbol{\varphi}_{ij}^{\mathrm{T}} \mathbf{u}_i(t). \tag{3}$$

For a 2D beam finite element, the local element stiffness matrix has three positive eigenvalues and three corresponding eigenvectors: axial distortion, bending distortion and shear/bending distortion.

2.2. Decomposition of the global elastic forces

Let $\mathbf{L}_i$ be the transformation matrix from the global co-ordinate system to the local co-ordinates of the ith element, so that

$$\mathbf{u}_i(t) = \mathbf{L}_i \mathbf{u}(t), \tag{4}$$

where $\mathbf{u}(t)$ is the displacement vector expressed in global coordinates. The global stiffness matrix $\mathbf{K}$ of the original undamaged structure can be assembled from local stiffness matrices as

$$\mathbf{K} = \sum_i \mathbf{L}_i^{\mathrm{T}} \mathbf{K}_i \mathbf{L}_i. \tag{5}$$

Thus, using Eqs. (1) to (4), the global elastic forces $\mathbf{K}\mathbf{u}(t)$ can be decomposed into a linear combination of total distortions $\kappa_{ij}(t)$ and the local nodal loads $\mathbf{n}_{ij}$:

$$\mathbf{K}\mathbf{u}(t) = \sum_i \mathbf{L}_i^{\mathrm{T}} \mathbf{K}_i \mathbf{u}_i(t) = \sum_{i,j} \kappa_{ij}(t) \mathbf{L}_i^{\mathrm{T}} \mathbf{n}_{ij}. \tag{6}$$

2.3. Modeling the modifications

Let $\mathbf{f}(t)$ be an external excitation and denote by $\mathbf{u}^{\mathrm{L}}(t)$ and $\kappa_{ij}^{\mathrm{L}}(t)$ the corresponding response of the unmodified structure. Using Eq. (6), the equation of motion can be stated as

$$\mathbf{M}\ddot{\mathbf{u}}^{\mathrm{L}}(t) + \mathbf{C}\dot{\mathbf{u}}^{\mathrm{L}}(t) + \sum_{i,j} \kappa_{ij}^{\mathrm{L}}(t) \mathbf{L}_i^{\mathrm{T}} \mathbf{n}_{ij} = \mathbf{f}(t). \tag{7}$$

Let the modeled damages of the structure be classified as

- mass-related, described in terms of a certain unknown modification $\Delta\mathbf{M}$ to the mass matrix, and
- stiffness-related, represented by uniform stiffness reductions of the affected finite elements and quantified by the ratio μ_i between the original local stiffness matrix $\mathbf{K}_i$ and the modified matrix $\tilde{\mathbf{K}}_i$,

$$\tilde{\mathbf{K}}_i = \mu_i \mathbf{K}_i. \tag{8}$$

The same external excitation $\mathbf{f}(t)$ as in Eq. (7), if applied to the damaged structure, results in the response $\mathbf{u}(t)$, as described by the following equation of motion:

$$(\mathbf{M} + \Delta\mathbf{M})\, \ddot{\mathbf{u}}(t) + \mathbf{C}\dot{\mathbf{u}}(t) + \sum_i \mathbf{L}_i^{\mathrm{T}} \left[\mathbf{K}_i - (1-\mu_i)\mathbf{K}_i\right] \mathbf{u}_i(t) = \mathbf{f}(t), \tag{9}$$

where Eq. (6) is used and the modifications are assumed not to influence considerably the damping properties of the structure. By moving the modification terms to the right-hand side and by Eq. (7), Eq. (9) can be rearranged into the equivalent form:

$$\mathbf{M}\ddot{\mathbf{u}}(t) + \mathbf{C}\dot{\mathbf{u}}(t) + \sum_{i,j} \kappa_{ij}(t)\mathbf{L}_i^{\mathrm{T}}\mathbf{n}_{ij} = \mathbf{f}(t) + \mathbf{p}^0(t) + \sum_{i,j} \kappa_{ij}^0(t)\mathbf{L}_i^{\mathrm{T}}\mathbf{n}_{ij}, \tag{10}$$

which is the equation of motion of the unmodified structure. In Eq. (10), the structural modifications are modeled by the pseudo-load $\mathbf{p}^0(t)$ and the virtual distortions $\kappa_{ij}^0(t)$, which are implicitly related to the response and the modifications by

$$\mathbf{p}^0(t) = -\Delta\mathbf{M}\ddot{\mathbf{u}}(t), \tag{11a}$$

$$\kappa_{ij}^0(t) = (1-\mu_i)\kappa_{ij}(t). \tag{11b}$$

Note that a virtual distortion $\kappa_{ij}^0(t)$ of a finite element can be identified with an additionally introduced time-dependent distortion. For simulation purposes, it is modeled with the corresponding vector $\kappa_{ij}^0(t)\mathbf{L}_i^{\mathrm{T}}\mathbf{n}_{ij}$ of self-equilibrated forces and moments that are applied in the DOFs of the involved element. Mass modifications are modeled by pseudo-loads $\mathbf{p}^0(t)$, which are unequilibrated loads applied in the involved DOFs.

2.4. Response of the damaged structure

Equation (10) confirms that structural damages and modifications can be modeled with the equivalent pseudo-loads and virtual distortions imposed on the original unmodified structure. This structure is assumed to satisfy Eq. (7) and so to be linear: potential nonlinearities, which can be for example related to the material (like plasticity) or to other types of damages (like breathing cracks), can be modeled using the same technique of virtual distortions, see [13, 28, 7]. Thus, the response of the damaged structure can be modeled as the following the sum of the responses of the original unmodified structure to the external excitation $\mathbf{f}(t)$, to the pseudo-loads $\mathbf{p}^0(t)$ and to the virtual distortions $\kappa_{ij}^0(t)$:

$$\ddot{\mathbf{u}}(t) = \ddot{\mathbf{u}}^{\mathrm{L}}(t) + \int_0^t \ddot{\mathbf{B}}^{\mathrm{up}}(t-\tau)\mathbf{p}^0(\tau)\,d\tau + \sum_{i,j}\int_0^t \ddot{\mathbf{B}}_{ij}^{\mathrm{u}\kappa}(t-\tau)\kappa_{ij}^0(\tau)\,d\tau, \tag{12a}$$

$$\kappa_{ij}(t) = \kappa_{ij}^{\mathrm{L}}(t) + \int_0^t \mathbf{B}_{ij}^{\kappa\mathrm{p}}(t-\tau)\mathbf{p}^0(\tau)\,d\tau + \sum_{k,l}\int_0^t B_{ijkl}^{\kappa\kappa}(t-\tau)\kappa_{kl}^0(\tau)\,d\tau, \tag{12b}$$

where the response to the pseudo-loads and virtual distortions are expressed through convolutions with the respective impulse-response functions of the original unmodified structure: $\ddot{\mathbf{B}}^{\mathrm{up}}(t)$, which is the matrix of acceleration responses in all DOFs to impulse excitations in all DOFs, $\ddot{\mathbf{B}}_{ij}^{\mathrm{u}\kappa}(t)$, which is the vector of acceleration responses in all DOFs to an impulsive unit distortion φ_{ij} (impulsive load $\mathbf{L}_i^{\mathrm{T}}\mathbf{n}_{ij}$), $\mathbf{B}_{ij}^{\kappa\mathrm{p}}(t)$, which is the response vector of the jth distortion of the ith finite element to impulse excitations in all DOFs, and $B_{ijkl}^{\kappa\kappa}(t)$, which is the response of the jth distortion of the ith finite element to an impulsive unit distortion φ_{kl} (impulsive load $\mathbf{L}_k^{\mathrm{T}}\mathbf{n}_{kl}$).

Equations (12) can be used to compute the response of the modified structure, provided the pseudo-loads and virtual distortions are known. However, Eqs. (11) state them in an implicit way, and so they cannot be used for a direct computation. Hence, Eqs. (12) are substituted in Eqs. (11) to obtain the following system

of Volterra integral equations:

$$-\Delta\mathbf{M}\ddot{\mathbf{u}}^{\mathrm{L}}(t) = \mathbf{p}^0(t) + \Delta\mathbf{M}\int_0^t \ddot{\mathbf{B}}^{\mathrm{up}}(t-\tau)\mathbf{p}^0(\tau)\,d\tau + \Delta\mathbf{M}\sum_{i,j}\int_0^t \ddot{\mathbf{B}}^{\mathrm{u}\kappa}_{ij}(t-\tau)\kappa^0_{ij}(\tau)\,d\tau, \tag{13a}$$

$$(1-\mu_i)\kappa^{\mathrm{L}}_{ij}(t) = \kappa^0_{ij}(t) - (1-\mu_i)\int_0^t \mathbf{B}^{\kappa\mathrm{p}}_{ij}(t-\tau)\mathbf{p}^0(\tau)\,d\tau - (1-\mu_i)\sum_{k,l}\int_0^t B^{\kappa\kappa}_{ijkl}(t-\tau)\kappa^0_{kl}(\tau)\,d\tau, \tag{13b}$$

where, apart from the unknowns $\mathbf{p}^0(t)$ and $\kappa^0_{ij}(t)$, all the other terms are known. For modifications small enough, Eqs. (13) are of the second kind and thus uniquely solvable [33]. Notice that, according to Eq. (11a), the pseudo-loads vanish in all DOFs that are not directly related to the mass modifications $\Delta\mathbf{M}$. Similarly, due to Eq. (11b), the virtual distortions are non-zero only in the modified finite elements. As a result, the dimension of the system Eq. (13) is significantly reduced, which makes numerical computations more feasible.

Equations (13) yield the pseudo-loads and virtual distortions, which are used in Eqs. (12) to compute the response of the modified structure. Alternatively, if the response of only a limited number of linear sensors (accelerometers, strain sensors, etc.) is required, the following formula can be used:

$$\mathbf{h}(t) = \mathbf{h}^{\mathrm{L}}(t) + \int_0^t \mathbf{B}^{\mathrm{hp}}(t-\tau)\mathbf{p}^0(\tau)\,d\tau + \sum_{i,j}\int_0^t \mathbf{B}^{\mathrm{h}\kappa}_{ij}(t-\tau)\kappa^0_{ij}(\tau)\,d\tau, \tag{14}$$

which relates the vector $\mathbf{h}(t)$ of the sensor responses in the modified structure to the corresponding responses $\mathbf{h}^{\mathrm{L}}(t)$ in the unmodified structure and to the pseudo-loads and virtual distortions that model the damage, see Eq. (10). Their effect is modeled using the corresponding impulse-responses $\mathbf{B}^{\mathrm{hp}}(t)$ and $\mathbf{B}^{\mathrm{h}\kappa}_{ij}(t)$ of the unmodified structure.

2.5. Discretization and solution

In practice, all the responses are either obtained via numerical simulations or measured and thus discrete. Therefore, the discrete counterparts of Eqs. (13) and (14) will be usually used. In the matrix notation, they take respectively the following forms of large linear equations:

$$\begin{bmatrix} -\Delta\mathbf{M}\ddot{\mathbf{u}}^{\mathrm{L}} \\ (1-\boldsymbol{\mu})\boldsymbol{\kappa}^{\mathrm{L}} \end{bmatrix} = \begin{bmatrix} \mathbf{I}+\Delta\mathbf{M}\ddot{\mathbf{B}}^{\mathrm{up}} & \Delta\mathbf{M}\ddot{\mathbf{B}}^{\mathrm{u}\kappa} \\ -(1-\boldsymbol{\mu})\mathbf{B}^{\kappa\mathrm{p}} & \mathbf{I}-(1-\boldsymbol{\mu})\mathbf{B}^{\kappa\kappa} \end{bmatrix} \begin{bmatrix} \mathbf{p}^0 \\ \boldsymbol{\kappa}^0 \end{bmatrix}, \tag{15}$$

$$\mathbf{h} = \mathbf{h}^{\mathrm{L}} + \begin{bmatrix} \mathbf{B}^{\mathrm{hp}} & \mathbf{B}^{\mathrm{h}\kappa} \end{bmatrix} \begin{bmatrix} \mathbf{p}^0 \\ \boldsymbol{\kappa}^0 \end{bmatrix}, \tag{16}$$

where the vectors $\ddot{\mathbf{u}}^{\mathrm{L}}$, $\boldsymbol{\kappa}^{\mathrm{L}}$, $\mathbf{h}$, $\mathbf{h}^{\mathrm{L}}$, $\mathbf{p}^0$ and $\boldsymbol{\kappa}^0$ are the discrete counterparts of the respective functions, collected for all involved DOFs, distortions and sensors; the matrices $\ddot{\mathbf{B}}^{\mathrm{up}}$, $\ddot{\mathbf{B}}^{\mathrm{u}\kappa}$, $\mathbf{B}^{\kappa\mathrm{p}}$, $\mathbf{B}^{\kappa\kappa}$, $\mathbf{B}^{\mathrm{hp}}$ and $\mathbf{B}^{\mathrm{h}\kappa}$ are the discrete counterparts of the respective Volterra matrix convolution operators, also collected for all involved DOFs, distortions and sensors; $\boldsymbol{\mu}$ is a block diagonal matrix of the respective dimension with the stiffness modification coefficients μ_i on the block diagonals.

For each assumed damage scenario, quantified by the mass and stiffness modifications $\Delta\mathbf{M}$ and μ_i, the equivalent pseudo-loads $\mathbf{p}^0$ and virtual distortions $\boldsymbol{\kappa}^0$ are obtained by solving Eq. (15). As it is a discretized version of a Volterra integral equation, it is usually significantly ill-conditioned and requires numerical regularization. Direct techniques (like the Tikhonov regularization) can be convenient for small problems, while iterative methods (like the conjugate gradient least squares, CGLS) are applicable for larger problems,

see [10, 34, 35]. Alternatively, the coefficient matrix can be rearranged into a lower triangular block matrix and solved stepwise by a block forward substitution. Besides the damage parameters $\Delta\mathbf{M}$ and μ_i, both equations contain only characteristics of the original undamaged structure. These characteristics can be sometimes directly measured [32], but more often they are pre-computed using a parametric numerical model of the undamaged structure (e.g. a FE model). In the latter case, the right-hand side of Eq. (15) contains results of numerical simulations not laden with measurement errors, which significantly reduces the negative effects of ill-conditioning. Solved Eq. (15), the response of sensors placed in the damaged structure is computed using Eq. (16). To this end, the solution is multiplied by a matrix, which (as a discrete counterpart of a convolution operator) acts as a smoothing operator that alleviates the effects of a potential under-regularization. As a result, the computed discrete response $\mathbf{h}$ of the damaged structure often turns out in practice to be stable for a wide range of regularization parameters.

Notice that, as Eqs. (15) and (16) contain only characteristics of the original undamaged structure, no modifications and no time-consuming repeated simulations of the structural model are necessary to account for the damages or modifications. This is an important advantage of the VDM-based structural reanalysis, which allows the identification of loads and damages to be performed quickly.

3. Identification of loads and damages

3.1. The direct problem

Equations (13) and (14), or their discrete counterparts Eqs. (15) and (16), can be used to compute the response of the damaged structure, provided that the external excitation $\mathbf{f}(t)$ is known or, more exactly, that the corresponding responses $\ddot{\mathbf{u}}^{\mathrm{L}}(t)$ and $\boldsymbol{\kappa}^{\mathrm{L}}(t)$ of the unmodified structure are known. In order to deal with the case of an unknown external excitation, it is initially assumed that the external excitation is impulsive, and the approach is used to compute the corresponding impulse-responses of the damaged structure. As the considered model of the damage preserves the linearity of the structure, the response of the damaged structure to any external excitation $\mathbf{f}(t)$ can be computed as the following convolution:

$$\mathbf{y}(t;\boldsymbol{\mu}^\star) = \int_0^t \mathbf{h}(t,\tau;\boldsymbol{\mu}^\star)\mathbf{f}(\tau)\,d\tau, \tag{17}$$

where the vector $\boldsymbol{\mu}^\star$ collects all the damage parameters (mass- and stiffness-related, as defined in Eq. (24) below), the vector $\mathbf{y}(t;\boldsymbol{\mu}^\star)$ collects the sensor responses, and the convolution kernel $\mathbf{h}(t,\tau;\boldsymbol{\mu}^\star)$ is the corresponding matrix of impulse-responses, which is stated here in the non-difference form to account for the possibility of moving loads (as in Sect. 4). The discretized version of Eq. (17) is expressed in the form

$$\mathbf{y}(\boldsymbol{\mu}^\star) = \mathbf{H}(\boldsymbol{\mu}^\star)\mathbf{f}, \tag{18}$$

where the matrix $\mathbf{H}(\boldsymbol{\mu}^\star)$ is the discrete counterpart of the integral operator in Eq. (17) and, with a proper ordering of the unknowns, takes the form of a block matrix with lower-triangular blocks, which are Toeplitz matrices in case of stationary loads. The vectors $\mathbf{y}(\boldsymbol{\mu}^\star)$ and $\mathbf{f}$ collect for all time steps respectively all the sensor responses and all the excitations. Notice that both the response and the convolution kernel explicitly depend on the vector $\boldsymbol{\mu}^\star$ of the damage parameters.

3.2. The inverse problem

If the damage of the structure is known, the external load can be identified by deconvolving the measured structural response $\mathbf{y}^{\mathrm{M}}(t)$ with respect to the known impulse-response. In practice, it is equivalent to solving the discrete linear equation

$$\mathbf{y}^{\mathrm{M}} = \mathbf{H}(\boldsymbol{\mu}^\star)\mathbf{f}(\boldsymbol{\mu}^\star), \tag{19}$$

which is basically feasible, provided the number of excitations does not exceed the number of sensors. However, if the damage is unknown, the impulse-response is also unknown and the identification problem

has to be formulated as a general minimization problem of the following objective function:

$$F(\mathbf{f}, \boldsymbol{\mu}^\star) = \frac{1}{2} \frac{\|\mathbf{y}^\mathrm{M} - \mathbf{H}(\boldsymbol{\mu}^\star)\mathbf{f}(\boldsymbol{\mu}^\star)\|^2}{\|\mathbf{y}^\mathrm{M}\|^2}. \tag{20}$$

Such an objective function depends simultaneously on excitations and structural parameters, which are two sets of unknowns with very different types, magnitudes and numbers. A standard optimization algorithm would treat all unknowns in the same way, which may lead to instabilities and significant inaccuracies. Thus, in the literature, either the types of the unknowns are unified before the optimization [26, 28] or a two-step optimization scheme is used to alternate between the unknowns of both types [24, 25]. Here, it is noted that, given the damage parameters, the corresponding excitation can be directly computed by a direct solution of Eq. (19),

$$\mathbf{f}(\boldsymbol{\mu}^\star) = \mathbf{H}^+(\boldsymbol{\mu}^\star)\mathbf{y}^\mathrm{M}, \tag{21}$$

where the superscript "+" denotes the pseudo-inverse, which formally accounts for the possible overdeterminacy of Eq. (19) and numerical regularization. Thus, the two-step approach is simplified into a standard problem of minimization of

$$F(\boldsymbol{\mu}^\star) = \frac{1}{2} \frac{\|\mathbf{y}^\mathrm{M} - \mathbf{y}(\boldsymbol{\mu}^\star)\|^2}{\|\mathbf{y}^\mathrm{M}\|^2}, \tag{22}$$

where the only unknowns are the damage parameters and

$$\mathbf{y}(\boldsymbol{\mu}^\star) = \mathbf{H}(\boldsymbol{\mu}^\star)\mathbf{H}^+(\boldsymbol{\mu}^\star)\mathbf{y}^\mathrm{M} \tag{23}$$

is the structural response estimated for the given damage parameters. Notice that the number of sensors must exceed the number of unknown excitations, otherwise the difference between the estimated and the measured responses would be entirely due to the ill-conditioning of Eq. (19) and would not contain any meaningful information about the damage.

However, even among the structural parameters, there still remains a considerable difference: a part of the optimization variables is related to mass modifications and form $\Delta\mathbf{M}$, while the other part consists of the dimensionless stiffness reduction coefficients $\boldsymbol{\mu}$, see Eq. (8). The magnitudes can be very disparate, which usually adversely affects the convergence and accuracy of the optimization process. In this case, the optimization can be improved by normalizing the mass-related variables, which are usually additional masses m_i, with respect to their initially estimated trial values m_i^tr. The trial values can be arbitrarily chosen based on the engineering experience. As a result, a set of normalized optimization variables of comparable magnitudes can be used, see also Eq. (8),

$$\mu_i^\star = \begin{cases} m_i/m_i^\mathrm{tr} & \text{if } i = 1, \ldots, n_\mathrm{m}, \\ \mu_{i-n_m} & \text{if } i = n_\mathrm{m}+1, \ldots, n_\mathrm{m}+n_\mathrm{e}, \end{cases} \tag{24}$$

where n_m and n_e are the numbers of mass- and stiffness-related damages respectively.

Note also that the computational cost of solving Eq. (19), and thus of all further operations involving the pseudo-inverse $\mathbf{H}^+(\boldsymbol{\mu}^\star)$, can be significantly reduced by employing a projection method [33]. The measurement time step is usually small and so the exact force time-history can be approximated by splines, wavelets, load shape functions [28], etc. Equation (19) takes then the following form:

$$\mathbf{y}^\mathrm{M} \approx \mathbf{H}(\boldsymbol{\mu}^\star)\mathbf{N}\boldsymbol{\alpha}(\boldsymbol{\mu}^\star), \tag{25}$$

where $\mathbf{f}(\boldsymbol{\mu}^\star) \approx \mathbf{N}\boldsymbol{\alpha}(\boldsymbol{\mu}^\star)$ and the approximating functions form the columns of the matrix $\mathbf{N}$. In this way, the unknown approximation coefficients $\boldsymbol{\alpha}(\boldsymbol{\mu}^\star)$ can be much fewer in number than the original unknowns $\mathbf{f}$.

3.3. Interpolation of structural responses and optimization

According to the above description, the main task in each optimization step is to estimate the system response Eq. (23). It requires the impulse-response matrix and its pseudo-inverse to be calculated, which

is computationally expensive. Moreover, the pseudo-inverse depends on the damage parameters in a non-obvious way, which makes the sensitivity analysis of $\mathbf{y}(\boldsymbol{\mu}^\star)$ hard to perform. Hence, a zero-order optimization approach based on interpolation of the structural response is used.

In each optimization step, the key procedure is to interpolate the relation between the structural response $\mathbf{y}(\boldsymbol{\mu}^\star + \Delta\boldsymbol{\mu}^\star)$ and the increment of the damage parameters $\Delta\boldsymbol{\mu}^\star$ using a linear combination of certain basis functions, which can be then used for a fast estimation of the response with regard to any given damage parameters. In practice, the function being interpolated is smooth, hence second-order polynomials are used. It is also assumed that the damage parameters influence the response independently from each other, which allows the number of interpolation points to be significantly reduced along with the computational cost of the interpolation. Thus, the ith element of the discrete response vector is interpolated in the vicinity of the point $\boldsymbol{\mu}^\star$ as follows:

$$y_i(\boldsymbol{\mu}^\star + \Delta\boldsymbol{\mu}^\star) \approx \tilde{y}_i(\boldsymbol{\mu}^\star + \Delta\boldsymbol{\mu}^\star) = y_i(\boldsymbol{\mu}^\star) + \sum_j a_{ij}\Delta\mu_j^\star + \sum_j b_{ij}(\Delta\mu_j^\star)^2, \tag{26}$$

where $\Delta\boldsymbol{\mu}^\star = [\Delta\mu_1^\star, \ldots, \Delta\mu_{n_\mathrm{m}+n_\mathrm{e}}^\star]$ is the modification vector. The interpolation coefficients a_{ij} and b_{ij} are computed, separately for each i and j, in the standard way by solving

$$\begin{bmatrix} \Delta\nu_{j1}^\star & (\Delta\nu_{j1}^\star)^2 \\ \Delta\nu_{j2}^\star & (\Delta\nu_{j2}^\star)^2 \end{bmatrix} \begin{bmatrix} a_{ij} \\ b_{ij} \end{bmatrix} = \begin{bmatrix} y_i(\boldsymbol{\mu}^\star + \Delta\nu_{j1}^\star\hat{\mathbf{e}}_j) - y_i(\boldsymbol{\mu}^\star) \\ y_i(\boldsymbol{\mu}^\star + \Delta\nu_{j2}^\star\hat{\mathbf{e}}_j) - y_i(\boldsymbol{\mu}^\star) \end{bmatrix}, \tag{27}$$

where $\hat{\mathbf{e}}_j$ denotes the unit vector colinear with the jth axis, while $\Delta\nu_{j1}^\star$ and $\Delta\nu_{j2}^\star$ are the interpolation steps along the same direction. The quadratic interpolation requires two steps in each direction and so a total of $1 + 2n_\mathrm{m} + 2n_\mathrm{e}$ interpolation points. Although this is not a small number, it is typical for zero-order optimization methods, which generally require repeated computations of the objective function in order to estimate its sensitivity with respect to the optimization variables. Here, the response and the objective function are characterized in a non-local way, and so the number of optimization steps is significantly reduced to just a few, as illustrated in the numerical and experimental examples below.

Equation (26) is substituted in Eq. (22). The resulting interpolation of the objective function,

$$F(\boldsymbol{\mu}^\star + \Delta\boldsymbol{\mu}^\star) \approx \tilde{F}(\boldsymbol{\mu}^\star + \Delta\boldsymbol{\mu}^\star) = \frac{1}{2}\frac{\sum_i \left[y_i^\mathrm{M} - \tilde{y}_i(\boldsymbol{\mu}^\star + \Delta\boldsymbol{\mu}^\star)\right]^2}{\sum_i \left(y_i^\mathrm{M}\right)^2}, \tag{28}$$

is a fourth-order polynomial, and so its first- and second-order derivatives can be easily computed and used in the optimization process, for example

$$\frac{\partial\tilde{F}(\boldsymbol{\mu}^\star + \Delta\boldsymbol{\mu}^\star)}{\partial\Delta\mu_k^\star} = \frac{\sum_i \left[y_i^\mathrm{M} - \tilde{y}_i(\boldsymbol{\mu}^\star + \Delta\boldsymbol{\mu}^\star)\right](-a_{ik} - 2b_{ik}\Delta\mu_k^\star)}{\sum_i \left(y_i^\mathrm{M}\right)^2}. \tag{29}$$

Notice that local and global accuracy of the interpolation can be weighted between by decreasing and increasing the interpolation steps. Larger interpolation steps result in a more wide distribution of the interpolation points (within predefined bounds on the damage parameters) and thus in an interpolation that captures more global characteristics of the objective function. Conversely, small interpolation steps yield an interpolation that is locally accurate. Thus, in the optimization process, the interpolation steps should be reduced as the search point approaches the minimum, which is implemented here by halving them in each iteration. Moreover, the accuracy of the interpolation can be verified at each iteration by comparing the interpolated and actual values of the objective function. If the accuracy is too low, an upper bound on the optimization step length can be introduced and controlled as in the Levenberg-Marquardt algorithm or other typical trust region approaches [36]. A schematic description of the general computational framework is shown in Fig. 1.

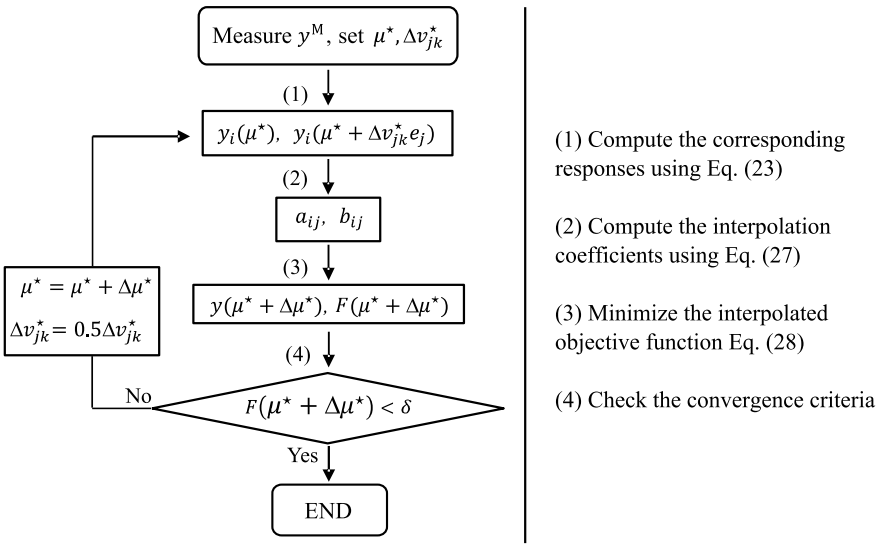

Figure 1: Simultaneous identification of excitations and damages. A schematic description of the general computational framework

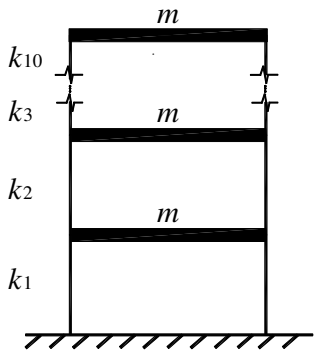

Figure 2: Numerical example. Ten-story building model

4. Numerical example

A numerical model of a ten-story building, Fig. 2, is used to verify the proposed method of simultaneous identification of excitations and damages. An idealized 10-DOF shear building model consisting of lumped masses and massless springs is used. The mass of each story is 4×10^5 kg and the shear stiffness of each story is 2×10^8 kN/m.

An additional mass of 1×10^5 kg is located on the second floor. Five randomly selected floors (2th, 4th, 5th, 7th and 9th) are damaged with the respective stiffness reduction ratios $\mu_2 = 0.4$, $\mu_4 = 0.7$, $\mu_5 = 0.9$, $\mu_7 = 0.6$ and $\mu_9 = 0.8$. Two acceleration transducers are placed on the 1st and 2nd floor. Earthquake wave "taft" (Fig. 3) is used as the excitation applied on the support of the structure. The corresponding dynamic responses of the two sensors are computed using the Newmark integration method with the standard parameters $\alpha = 0.25$ and $\beta = 0.5$. The integration step equals 0.01 s, thus the sampling frequency is 100 Hz. A total of 1600 time steps are used, which corresponds to the sampling time interval of 16 s. The simulated sensor responses are shown in Fig. 4.

In order to verify the VDM-based reanalysis method, discrete impulse responses of the damaged system have been computed using the VDM via Eq. (15) and Eq. (16). The responses have been computed with respect to impulsive excitations applied at the support and compared to the impulse responses computed

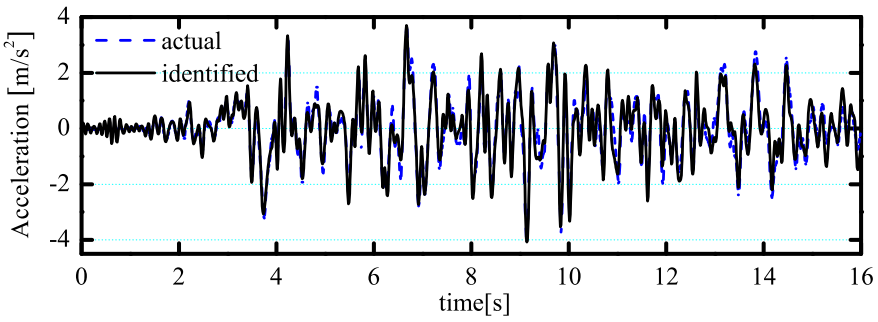

Figure 3: Numerical example. Comparison of the actual and identified excitations

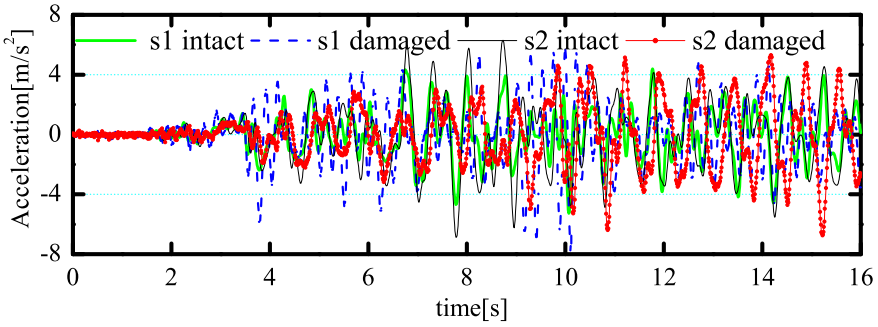

Figure 4: Numerical example. Simulated responses of the damaged and intact systems

using a directly updated FE model of the damaged structure. The relative root mean square errors were at the level of numerical errors (10^{-10} to 10^{-9}), which attests the accuracy of the VDM-based approach.

For identification purposes, it is assumed that the stiffness of all the stories can be damaged, so that ten stiffness reduction coefficients are used in optimization, besides the unknown additional mass and the excitation. Altogether, there are 11 damage parameters and the time-history of the earthquake wave that need to be identified. The measured data is contaminated with a numerically generated uncorrelated Gaussian noise at 5% rms level. The optimization is performed using the zero-order interpolation approach described in Sect. 3.3. The trial mass value is set as 2×10^5 kg. The initial values of all the optimization variables are set to be 1, that is, the optimization starts from the intact structure with the trial mass. The stiffness-related damage parameters belong to the interval $(0, 1]$, while the mass-related parameter is only bounded from below by 0. Thus, the initial interpolation steps are set for all the variables as $\Delta\nu^\star_{i1} = -0.45$ and $\Delta\nu^\star_{i2} = -0.9$. These values are halved in each successive iteration.

Fig. 5 shows the identified damage parameters. With 5% noise pollution, both damage extents and their locations are identified precisely. The fast convergence of the interpolation-based optimization algorithm is illustrated in Fig. 6, which plots the values of the eleven optimization variables in all iterations. Fig. 3 compares the actual excitation to the identified loads; the accuracy is acceptable. To reduce the numerical costs and improve the numerical conditioning of the identification, the identification of the excitation is carried out efficiently in a moving time window [28]. All the 1600 time steps are divided into 8 sections of 200 time steps with the overlapping parts of 100 time steps. In each section, the excitation has been approximated, as described in Eq. (25), by a linear combination of forty two load shape functions, which are constructed from standard shape functions of a frame element.

The program is implemented using Matlab and a standard PC desktop computer. To asses the efficiency of the proposed numerical procedures, two additional tests are carried out:

1. The whole identification takes 34 s. Without the VDM and without the interpolation of the structural response, the computation time increases to 52 s.

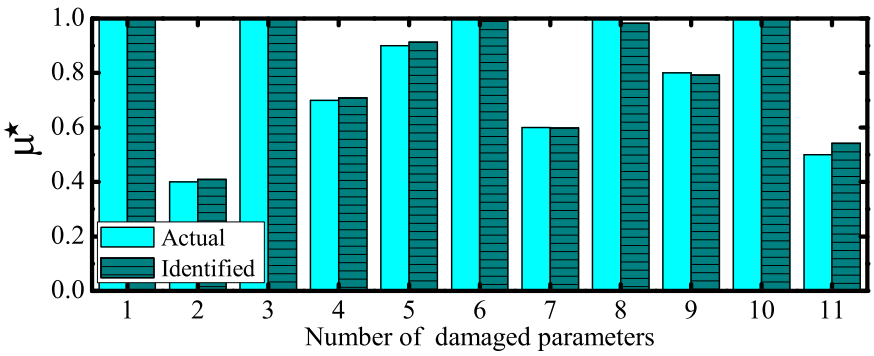

Figure 5: Numerical example. Comparison of the identification results

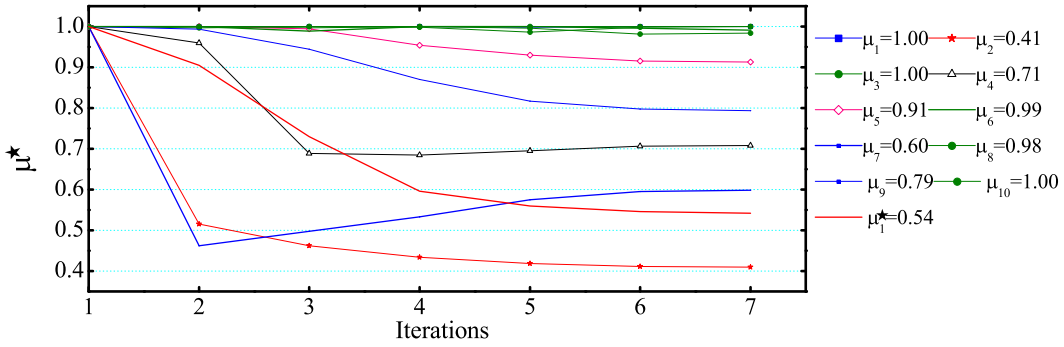

Figure 6: Numerical example. The optimization variables in successive optimization steps: μ_1 to μ_{10} are the stiffness-related parameters, while $\mu_1^\star$ is the normalized mass-related parameter, see Eq. (24)

2. Computation of the excitation via Eq. (23) takes 0.15 s and is the most time-consuming operation. Without the technique of the moving time window and without the approximation by the load shape functions, the computation time increases to 8 s.

5. Experimental verification

5.1. The structure

The experimental setup is shown in Fig. 7. The specimen, an aluminum cantilever beam, has the length of 136.15 cm, and a rectangular cross-section 2.7 cm × 0.31 cm. The fixed end is clamped to a stable frame. Young's modulus of the beam is 70 GPa, and the density is 2700 kg/m^3. The beam is slender, thus the gravity is considered in its FE model, as well as the influence of the piezoelectric actuator and strain sensors. A segment of the beam is damaged by cutting even notches, see Fig. 7, on the length of 10.23 cm near the fixed end. The stiffness of the damaged segment is decreased to 42% of the original stiffness, while the mass is left nearly unchanged. Moreover, an additional mass block with the weight of 60 g is screwed on the beam near the free end.

5.2. Excitations and measurements

The excitation is applied using an Amplified Piezo Actuator (APA, a solid-state long-stroke linear actuator), which is fixed on the beam in such a way that it can be assumed to apply a pure moment load. The dynamic structural responses are measured using three piezoelectric patches, which are glued to the beam to measure the structural strain. The sampling frequency is chosen to be 2500 Hz in order to guarantee that no important dynamic information is lost in the sampling process. Three kinds of dynamic

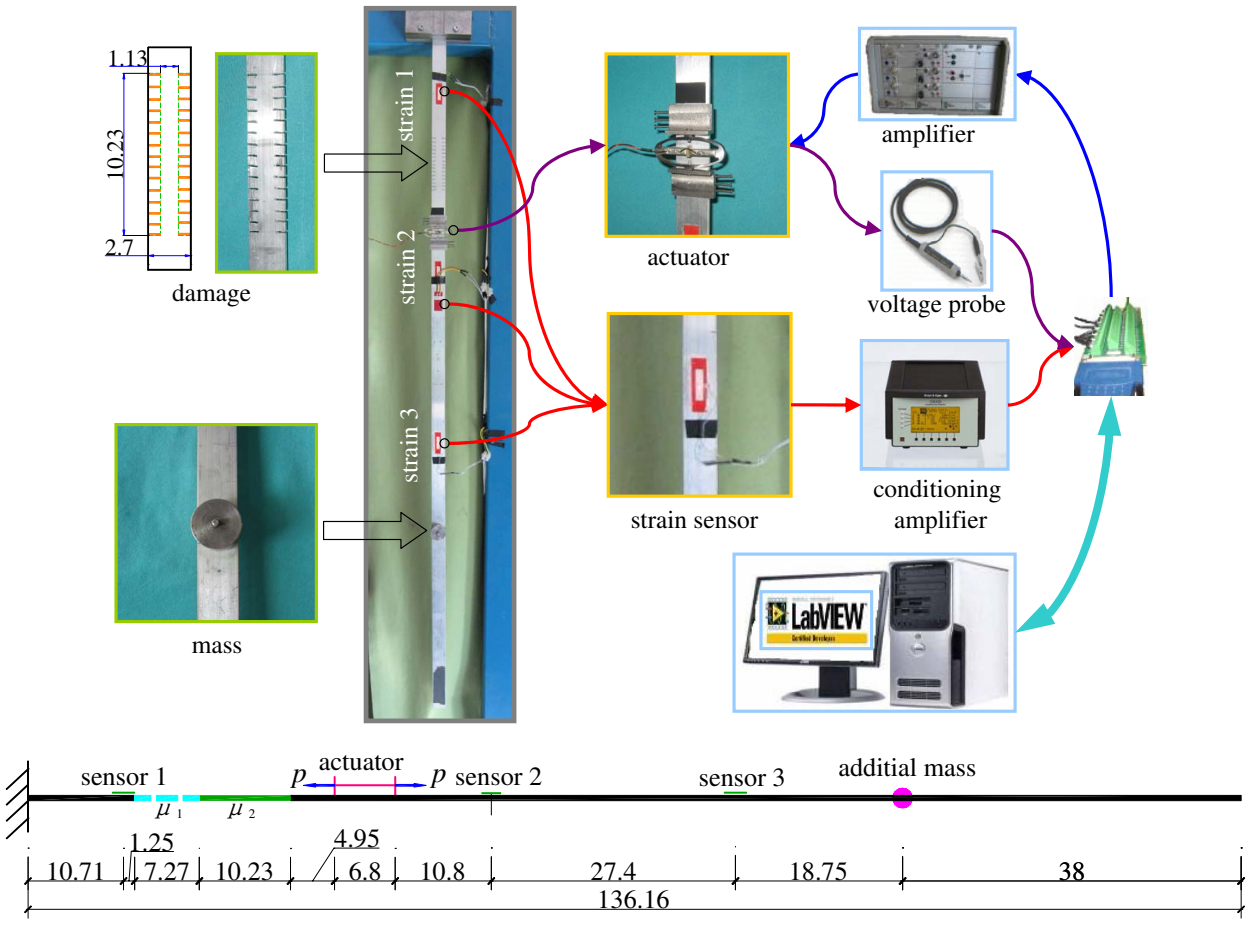

Figure 7: Experimental setup

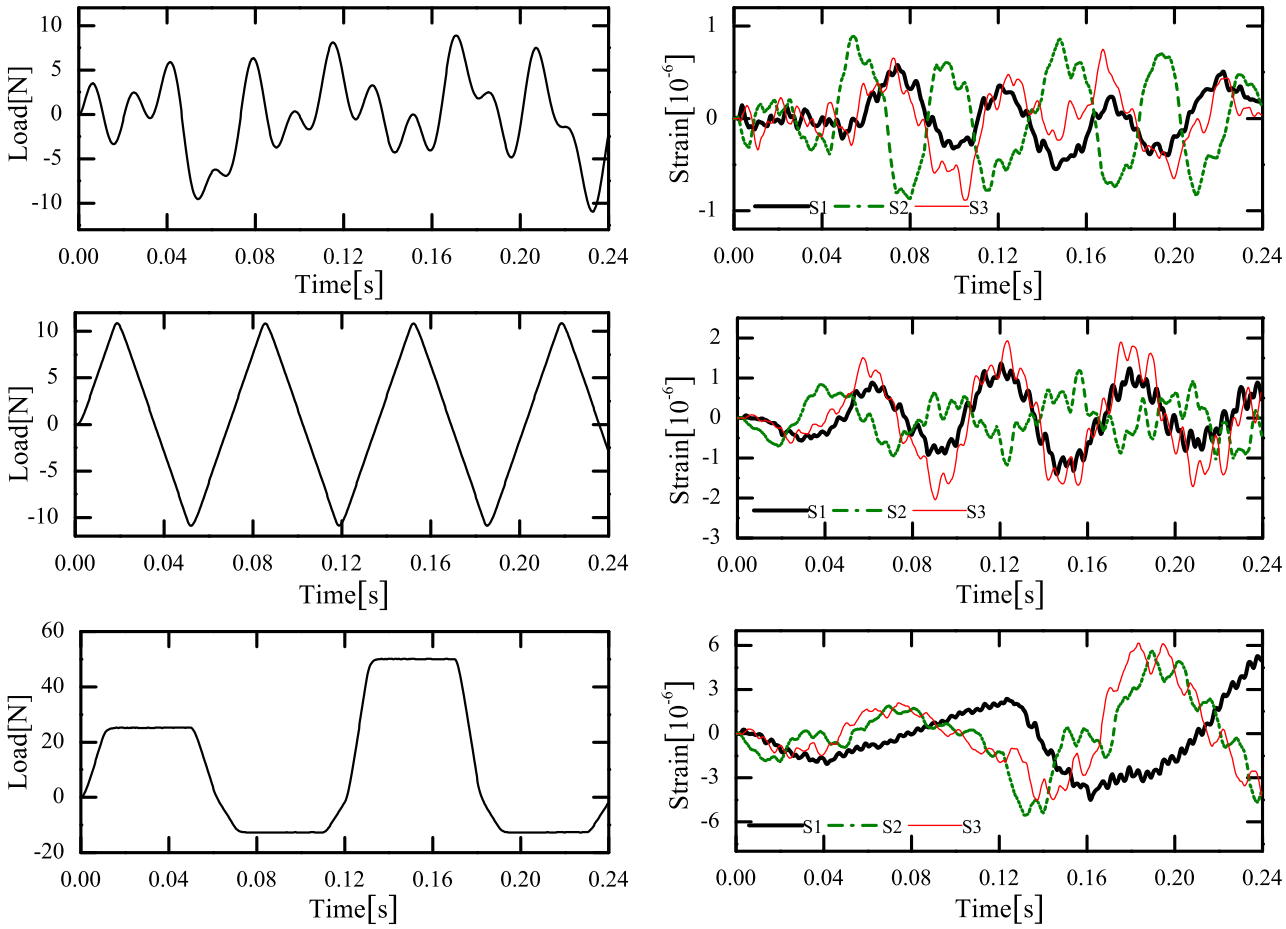

Figure 8: Experimental example. (*left*) excitations, (*right*) responses; (*top*) Case 1: continuous excitation, (*middle*) Case 2: triangular excitation, (*bottom*) Case 3: quasi-rectangular excitation

excitations, see Fig. 8 (left), are designed and separately applied. The measurement time interval is 0.24 s, so that there are 600 time steps.

5.3. Simultaneous identification of loads and damages

It is assumed that there are two potential unknown stiffness-related damages: μ_1 of the beam segment between sensor 1 and the damaged segment, and μ_2 of the damaged segment. Therefore, three damage parameters (two stiffness-related and one mass-related) and one excitation are unknown and need to be identified. The optimization variable related to the mass is normalized with respect to the trial value, see Eq. (24). The estimation based on the intact structure and direct identification of the pseudo-loads yields a negative value, possibly due to the significant effects of the damages, so the unit value of 1 kg has been used as the trial mass value. In the first optimization iteration, the initial values of the three normalized damage parameters are set as $(1, 1, 0)$, which means that the optimization starts from the intact structure. The interpolation steps in the first iteration are $(-0.45, -0.9)$ for the stiffness-related parameters and $(0.45, 0.9)$ for the mass-related parameter; these values are halve in each successive iteration.

Table 1 lists the identified damage parameters for the three considered cases, which differ by the applied excitations. As in the numerical example, mass identification results are assessed by their relative accuracy, while the identified stiffness reduction ratios are assessed by their absolute accuracy (percentage points). The stiffness reduction ratios are identified precisely: the errors are less than 5.7% (and 3% on average)

Table 1: Experimental example. Identification results

		Case 1		Case 2		Case 3	
	actual	identified	error (%)	identified	error (%)	identified	error (%)
μ_1	1.00	0.972	2.83	0.979	2.06	1.028	2.83
μ_2	0.42	0.416	0.43	0.477	5.69	0.46	4.00
m (10^3 kg)	0.06	0.058	2.67	0.058	3.83	0.059	2.33

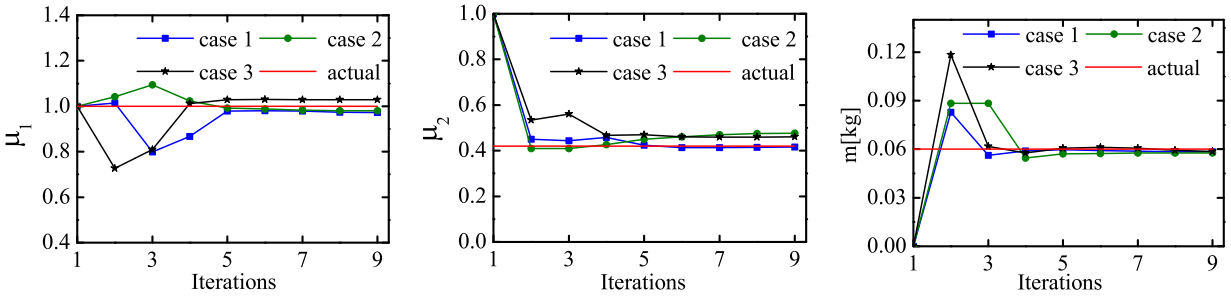

Figure 9: Experimental example. Damage parameters in successive optimization steps

under all three kinds of excitation; the damage location (limited to the two considered beam segments) can be judged by the identified damage extent. The additional mass is also identified accurately (up to 3.9% relative error). The values of the damage parameters in all iterations are plotted in Fig. 9, which confirms that the results can be quickly achieved in just a few iterations.

The identification of the excitation is performed, as in the numerical example, in a moving time window. In all three cases, 600 time steps are divided into eleven sections of 100 time steps with the overlapping parts of 50 time steps. In each section, the excitation is identified by using an approximation by twenty load shape functions and Eq. (25). The final identified excitations are plotted in Fig. 10. The continuous and triangular excitations are identified properly, while the identification accuracy for the quasi-rectangular excitation is slightly worse, as the amplitude is a little overestimated.

6. Conclusions

This paper has proposed and experimentally verified a methodology for simultaneous identification of unknown excitations and damages. Contrary to other approaches, damage-related parameters are treated as the only optimization variables, while the corresponding unknown excitation is uniquely determined based on the measured response. As a result, there is no type difference among the optimization variables, which allows standard optimization approaches to be used. In each optimization step, the structural response is interpolated with respect to the damage parameters, which increases the computational efficiency and facilitates sensitivity analysis. The impulse responses of the modified structure are quickly computed using the virtual distortion method (VDM).

The methodology is verified experimentally using an aluminum cantilever beam. Three sensors are used to identify three structural parameters and an unknown excitation. The identification error depends on the time-history of the excitation; in all tested cases it is less than 2.9% (for the two stiffness-related parameters) or 8.2% (for the mass-related parameter).

The research is ongoing to include other types of damages as well as to consider online identification.

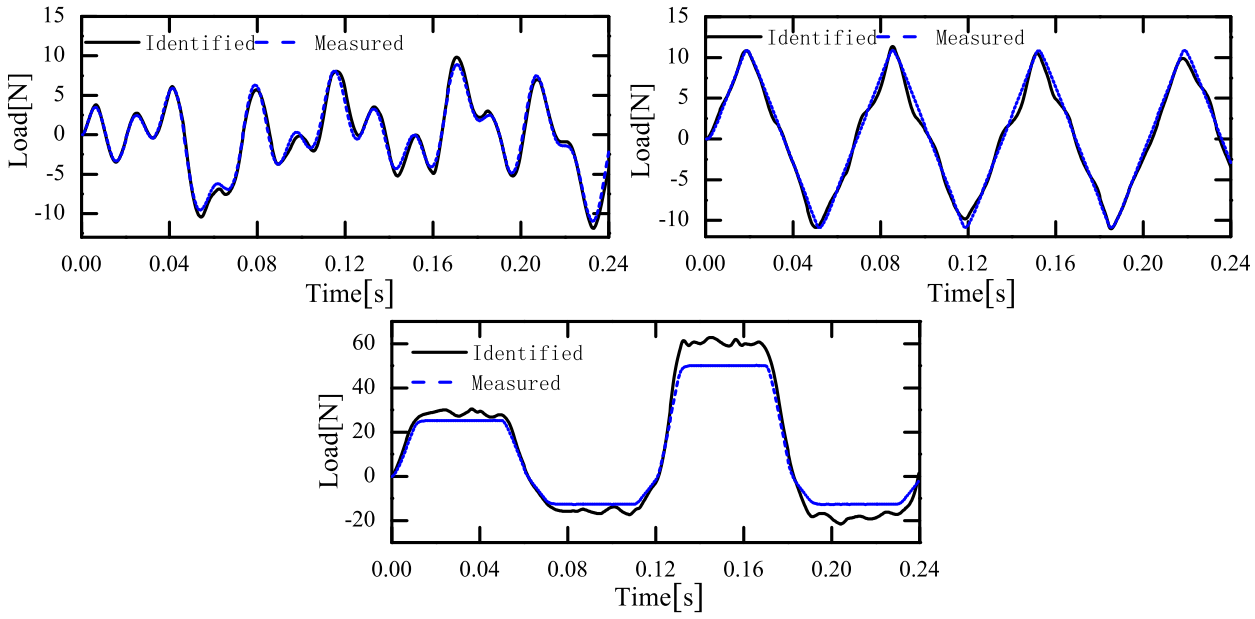

Figure 10: Experimental example. Comparison of the actual and identified excitations: (*top left*) Case 1; (*top right*) Case 2; (*bottom*) Case 3

7. Acknowledgement

Financial support of Structural Funds in the Operational Programme – Innovative Economy (IE OP) financed from the European Regional Development Fund – Projects "Modern material technologies in aerospace industry" (POIG.0101.02-00-015/08) and "Smart technologies for safety engineering — SMART and SAFE" (TEAM/2008-1/4, operated within the Foundation for Polish Science Team Programme) is gratefully acknowledged. This research is partially supported by the China National Natural Science Foundation under Grants #50579008 and #51108066.

References

[1] W.J. Staszewski, Structural Health Monitoring using Guided Ultrasonic Waves, in: J. Holnicki-Szulc, C.A. Mota Soares (Eds.), Advances in Smart Technologies in Structural Engineering, Springer, 2003, pp. 117-162.

[2] W. Ostachowicz, P. Kudela, P. Malinowski, T. Wandowski, Damage localisation in plate-like structures based on PZT sensors, Mechanical Systems and Signal Processing 23 (6) (2009) 1805–1829.

[3] S. Silva, M. Dias Júnior, V. Lopes Jr., Structural Health Monitoring in Smart Structures Through Time Series Analysis, Structural Health Monitoring 7 (3) (2008) 231–244.

[4] J. Holnicki-Szulc (ed.), Smart Technologies for Safety Engineering, John Wiley & Sons, Chichester, 2008.

[5] G. Yan, Structural damage identification methods based on generalized flexibility matrix and wavelet analysis, PhD thesis, School of Civil Engineering, Harbin Institute of Technology, 2006.

[6] S.W. Doebling, C.R. Farrar, M.B. Prime, A Summary Review of Vibration-Based Damage Identification Methods, The Shock and Vibration Digest 30 (2) (1998) 91–105.

[7] P. Kołakowski, M. Wikło, J. Holnicki-Szulc, The virtual distortion method — a versatile reanalysis tool for structures and systems, Structural and Multidisciplinary Optimization 36 (3) (2008) 217–234.

[8] L.E. Mujica, J. Vehí, W. Staszewski, K. Worden, Impact damage detection in aircraft composites using knowledge-based reasoning, Structural Health Monitoring 7 (3) (2008) 215–230.

[9] H. Inoue, J.J. Harrigan, S.R. Reid, Review of inverse analysis for indirect measurement of impact force, Applied Mechanics Reviews 54 (6) (2001) 503–524.

[10] E. Jacquelin, A. Bennani, P. Hamelin, Force reconstruction: analysis and regularization of a deconvolution problem, Journal of Sound and Vibration 265 (1) (2003) 81–107.

[11] T. Uhl, The inverse identification problem and its technical application, Archive of Applied Mechanics 77 (5) (2007) 325–337.

[12] R. Adams, J.F. Doyle, Multiple force identification for complex structures, Experimental Mechanics 42 (1) (2002) 25–36.

[13] Ł. Jankowski, Off-line identification of dynamic loads, Structural and Multidisciplinary Optimization 37 (6) (2009) 609–623.
[14] S. Ödeen, B. Lundberg, Prediction of impact force by impulse response method, International Journal of Impact Engineering 11 (2) (1991) 149–158.
[15] H. Inoue, H. Ishida, K. Kishimoto, T. Shibuya, Measurement of impact load by using an inverse analysis technique: Comparison of methods for estimating the transfer function and its application to the instrumented Charpy impact test, Japan Society of Mechanical Engineers International Journal 34 (4) (1991) 453–458.
[16] J.F. Doyle, A wavelet decmnvolution method for impact force identification, Experimental Mechanics 37 (4) (1997) 403–408.
[17] Q.P. Ha, H. Trinh, State and input simultaneous estimation for a class of nonlinear systems, Automatica 40 (10) (2004) 1779–1785.
[18] M. Klinkov, C.P. Fritzen, An updated comparison of the force reconstruction methods, Key Engineering Materials 347 (2007) 461–466.
[19] M.S. Allen, T.G. Carne, Comparison of inverse structural filter (ISF) and sum of weighted accelerations technique (SWAT) time domain force identification methods, In: 47th AIAA/ASME/ASCE/AHS/ASC Structures, Structural Dynamics, and Materials Conference, Newport, RI, 2006.
[20] M.S. Allen, T.G. Carne, Delayed, multi-step inverse structural filter for robust force identification, Mechanical Systems and Signal Processing, 22 (5) (2008) 1036–1054.
[21] J.J. Liu, C.K. Ma, I.C. Kung, D.C. Lin, Input force estimation of a cantilever plate by using a system identification technique, Computer Methods in Applied Mechanics and Engineering 190 (11–12) (2000) 1309–1322.
[22] X. Cao, Y. Sugiyamac, Y. Mitsui, Application of artificial neural networks to load identification, Computers and Structures 69 (1) (1998) 63–78.
[23] J. Chen, J. Li, Simultaneous identification of structural parameters and input time history from output-only measurements, Computational Mechanics 33 (5) (2004) 365–374.
[24] X.Q. Zhu, S.S. Law, Damage detection in simply supported concrete bridge structure under moving vehicular loads, Journal of Vibration and Acoustics 129 (1) (2007) 58–65.
[25] Z.L. Lu, S.S. Law, Identification of system parameters and input force from output only, Mechanical Systems and Signal Processing 21 (5) (2007) 2099–2111.
[26] K. Zhang, H. Li, Z. Duan, S.S. Law, A probabilistic damage identification approach for structures with uncertainties under unknown input, Mechanical Systems and Signal Processing 25 (4) (2011) 1126–1145.
[27] M. Hoshiya, O. Maruyama, Identification of running load and beam system, Journal of Engineering Mechanics ASCE 113 (6) (1987) 813–824.
[28] Q. Zhang, Ł. Jankowski, Z. Duan, Simultaneous identification of moving masses and structural damage, Structural and Multidisciplinary Optimization 42 (6) (2010) 907–922.
[29] Q. Zhang, Ł. Jankowski, Z. Duan, Identification of coexistent load and damage, Structural and Multidisciplinary Optimization, 41 (2) 2010 (243–253).
[30] A. Świercz, P. Kołakowski, J. Holnicki-Szulc, Damage identification in skeletal structures using the virtual distortion method in frequency domain, Mechanical Systems and Signal Processing 22 (8) (2008) 1826–1839.
[31] M.A. Akgün, J.H. Garcelon, R.T. Haftka, Fast exact linear and non-linear structural reanalysis and the Sherman-Morrison-Woodbury formulas, International Journal for Numerical Methods in Engineering 50 (7) (2001) 1587–1606.
[32] G. Suwała, Ł. Jankowski, A model-free method for identification of mass modifications, Structural Control & Health Monitoring 19 (2) (2012) 216–230.
[33] R. Kress, Linear integral equations, 2nd ed., Springer, New York, 1999.
[34] P.C. Hansen, Discrete inverse problems: insight and algorithms, SIAM, Philadelphia, 2010.
[35] Å. Björck, Numerical Methods in Scientific Computing, vol. 2. SIAM, Philadelphia, 2010.
[36] J. Nocedal, S.J. Wright, Numerical optimization, 2nd ed., Springer, 2006.